Environmental Science & Technology

Article

pubs.acs.org/est

Hydroquinone-Mediated Redox Cycling of Iron and Concomitant Oxidation of Hydroquinone in Oxic Waters under Acidic Conditions: Comparison with Iron−Natural Organic Matter Interactions

Chao Jiang, Shikha Garg, and T. David Waite*

School of Civil and Environmental Engineering, The University of New South Wales, Sydney, NSW 2052, Australia

Supporting Information

ABSTRACT: Interactions of 1,4-hydroquinone with soluble iron species over a pH range of 3−5 in the air-saturated and partially deoxygenated solution are examined here. Our results show that 1,4-hydroquinone reduces Fe(III) in acidic conditions, generating semiquinone radicals ($Q^{\bullet-}$) that can oxidize Fe(II) back to Fe(III). The oxidation rate of Fe(II) by $Q^{\bullet-}$increases with increase in pH due to the speciation change of $Q^{\bullet-}$ with its deprotonated form ($Q^{\bullet-}$) oxidizing Fe(II) more rapidly than the protonated form ($HQ^{\bullet}$). Although the oxygenation of Fe(II) is negligible at pH < 5, O_2 still plays an important role in iron redox transformation by rapidly oxidizing $Q^{\bullet-}$ to form benzoquinone (Q). A kinetic model is developed to describe the transformation of quinone and iron under all experimental conditions. The results obtained here are compared with those obtained in our previous studies of iron−Suwannee River fulvic acid (SRFA) interactions in acidic solutions and support the hypothesis that hydroquinone moieties can reduce Fe(III) in natural waters. However, the semiquinone radicals generated in pure hydroquinone solution are rapidly oxidized by dioxygen, while the semiquinone radicals generated in SRFA solution are resistant to oxidation by dioxygen, with the result that steady-state semiquinone concentrations in SRFA solutions are 2−3 orders of magnitude greater than in solutions of 1,4-hydroquinone. As a result, semiquinone moieties in SRFA play a much more important role in iron redox transformations than is the case in solutions of simple quinones such as 1,4-hydroquinone. This difference in the steady-state concentration of semiquinone species has a dramatic effect on the cycling of iron between the +II and +III oxidation states, with iron turnover frequencies in solutions containing SRFA being 10−20 times higher than those observed in solutions of 1,4-hydroquinone.

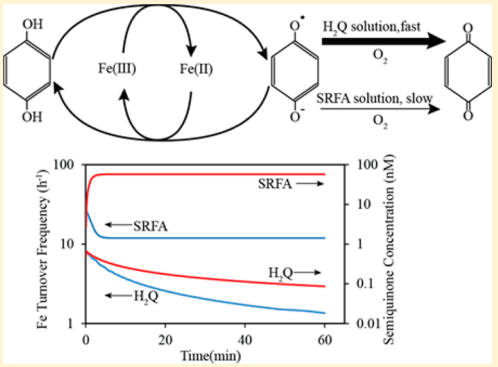

1. INTRODUCTION

Quinone moieties are common in natural aquatic environments and in biological systems and play a key role in the electron-transfer processes. The term "quinones" refers collectively to organic structures in three oxidation states: the fully reduced hydroquinone (H_2Q), the intermediate semiquinone radical ($Q^{\bullet-}$), and the fully oxidized quinone (Q). The redox properties of natural organic matter (NOM) have been associated with quinone moieties, with the presence of these moieties in NOM confirmed by NMR,[1] fluorescence spectroscopy,[2,3] and electrochemical methods.[4] These quinone moieties are implicated in a wide range of redox active processes including generating reactive oxygen species (ROS),[5] degradation of organic contaminants, and, potentially, mediating redox transformation of metals such as iron[6] and copper.[7]

Our recent studies on redox transformations of iron by Suwannee River fulvic acid (SRFA) under acidic conditions in the dark have shown that Fe(III) reducing hydroquinone-like moieties ($pK_a > 7$) are present intrinsically in SRFA, with these moieties oxidizing to relatively long-lived semiquinone-like radicals ($pK_a \approx 4.1$) on irradiation that serve as Fe(II) oxidants under acidic conditions.[8,9] In this study, we investigate the kinetics and mechanism of the iron redox transformation in pure hydroquinone solution in the pH range of 3−5 in air-saturated and partially deoxygenated solution with the goal of identifying the similarities and differences between this simple quinone and the quinone moieties present in SRFA. Despite the similarities that might be expected between the redox behavior of pure quinones and SRFA, major differences are also likely. For example, SRFA consists of an extended network of potentially conjugated aromatic structures leading to the possibility of stabilization of radicals.[10,11] Such an effect will not occur with a simple hydroquinone. Furthermore, in the hydroquinone solution, iron will be present in inorganic form while in SRFA solution, iron (especially Fe(III)) will be complexed by SRFA. The effect of these differences in SRFA and hydroquinone properties on Fe redox transformation is discussed within the context of the experimental results obtained here. Although there are many different hydroquinones, we focus here on the simplest, 1,4-hydroquinone ($pK_{a1} = 10.2$; $pK_{a2} = 12.0$) and its oxidized forms (semiquinone

Received: July 1, 2015
Revised: November 14, 2015
Accepted: November 18, 2015
Published: November 18, 2015

DOI: 10.1021/acs.est.5b03189
Environ. Sci. Technol. 2015, 49, 14076−14084

radical (pK_a = 4.1) and 1,4-benzoquinone) because no direct binding of iron by this organic compound is expected. Note that 1,4 hydroquinone is not representative of quinones in general but is being used as an example of a simple quinone. The pH is constrained in the range of 3−5 to be consistent with our previous studies in SRFA solutions.[9] Under acidic conditions, oxygenation of both Fe(II) and hydroquinone are expected to be negligible; as such, it is possible to investigate the Fe(III)-mediated oxidation of hydroquinone as well as hydroquinone-mediated Fe(III) redox transformations.

2. EXPERIMENTAL METHODS

2.1. Reagents. All solutions were prepared using 18 MΩ·cm resistivity Milli-Q water unless stated otherwise. All glass- and plastic-ware was soaked in 5% HCl for at least 24 h prior to use. Buffer solutions at pH 3, 4, 4.5, and 5 contained 10 mM NaCl (Sigma) and appropriate amounts of HCl (high purity 30% w/v; Sigma). These solutions were air-saturated by being allowed to equilibrate overnight with the atmosphere. All pH measurements were carried out using a calibrated Hanna 210 pH meter, with pH adjustments performed using 1 M HCl or 1 M NaOH (Sigma) solutions. A maximum pH variation of ±0.1 units was allowed. All stock solutions were stored at 4 °C when not in use unless stated otherwise.

A primary stock solution of 40 mM 1,4-hydroquinone (Sigma) in 5 mM HCl was prepared daily. A working stock solution containing 2 mM H_2Q in 0.25 mM HCl was prepared by a 20× dilution of the primary stock solution. Stock solutions of Fe(II), Fe(III), H_2O_2, ferrozine (3-(2-pyridyl)-5,6-diphenyl-1,2,4-triazine-4′,4″-disulfonic acid sodium salt; abbreviated as FZ hereafter; Fluka), desferrioxamine B (DFB; Sigma), amplex red (AR; Invitrogen), horseradish peroxidase (HRP; Sigma), and superoxide dismutase (SOD; Sigma) were prepared and stored as reported in our earlier work[9] and as also described in the Supporting Information. The concentration of Fe(III) used in our experiments is below the solubility limit of Fe(III) at the pH values investigated here, and hence, all Fe(III) added was present as dissolved inorganic Fe(III) species.

Because superoxide mostly exists as $HO_2^{\bullet}$ in the pH range investigated, we use $HO_2^{\bullet}$ to represent superoxide from here on in our discussion. Also, Fe(III) and Fe(II) are used to represent total inorganic iron in +III and +II oxidation states, respectively.

2.2. Experimental Setup. All experiments were performed in air−saturated buffer solution at a temperature of 22 °C unless stated otherwise. To study the reaction of H_2Q and Fe(III), we added appropriate concentrations of H_2Q and Fe(III) stock solutions to the 30 mL air-saturated buffer placed in plastic bottles covered with aluminum foil to avoid interference from outside light. Samples were withdrawn from the reactor continuously using a peristaltic pump for Q measurement or manually every 10 min for Fe(II) and H_2O_2 measurement. No filtration of samples was required prior to analysis because no solid was present in our experimental matrix. To determine the role of dioxygen in the experimental system investigated here, we conducted one set of experiments in which the concentration of dioxygen was reduced by sparging the buffered solution with argon in a sealed reactor for 4 h prior to experiments. The concentration of dioxygen was reduced to 5−10% of the initial dioxygen concentration in our solution (complete oxygen removal was very difficult to achieve). Sparging was continued during the experiments. Samples were withdrawn from the sealed reaction vessel using fine tubing connected to either a peristaltic pump (for Q measurement) or a syringe (for Fe(II) and H_2O_2 measurement) without opening the sealed reactor. An estimate of the dioxygen concentration in the sparged solution was obtained by measuring the rate of inorganic Fe(II) oxidation in a pH 8 buffered solution sparged in an identical manner to the solutions of interest.

2.3. Measurement of Fe(II). The concentration of Fe(II) generated on reduction of Fe(III) was determined using a modified FZ method as described in our earlier work.[8] A molar absorption coefficient of 2.6 × 10^4 M^{-1} cm^{-1} at 562 nm for $Fe(FZ)_3$ was obtained for all experimental conditions investigated here, which is close to the value reported by Stookey.[12]

2.4. Measurement of Benzoquinone. The concentration of benzoquinone formed on the oxidation of hydroquinone was determined by measuring its UV absorbance at 247 nm using a 1 m path-length type II liquid waveguide capillary cell (World Precision Instruments) connected with broadband deuterium−halogen lamp as the light source and a USB 4000 spectrophotometer (Ocean Optics). A molar absorption coefficient of 1.8× 10^4 M^{-1} cm^{-1} was obtained, which is close to the reported value of 2.1 × 10^4 M^{-1} cm^{-1}.[13]

2.5. Measurement of H_2O_2. H_2O_2 concentrations generated on H_2Q and Fe(III) reaction were determined fluorometrically using 2 μM AR and 1 $kU{\cdot}L^{-1}$ HRP as the fluorescence reagent.[14] The procedure and settings used for measurement on a Cary Eclipse fluorescence spectrophotometer (Agilent Technologies) have been described previously.[15]

2.6. Kinetic Modeling. The software package Kintecus[16] was used for kinetic modeling of the experimental results. Sensitivity analysis of the kinetic model was performed by calculating normalized sensitivity coefficients (NSCs) and undertaking principal component analysis (PCA) as described by Vajda and co-workers.[17] The NSCs were calculated using Kintecus while PCA was performed using MATLAB.

3. RESULTS AND DISCUSSION

3.1. Fe(II) Generation on Fe(III) Reduction by Hydroquinone. When Fe(III) was added to air-saturated hydroquinone solution at pH 4, the Fe(II) concentration increased as a result of Fe(III) reduction by hydroquinone (Figure 1a). The Fe(II) concentration increased rapidly initially; however, the Fe(II) generation rate slowed down over time. Because the generation rate of Fe(II) decreases over time with the Fe(II) concentration approaching steady-state (especially at higher concentrations of H_2Q), it appears that back-oxidation of Fe(II), formed as a result of Fe(III) reduction, also occurs. Because negligible Fe(II) oxidation occurs by reaction with dioxygen at pH 4 (at least over the time scale of interest; see Figure S1), this observation further suggests that one or more of the quinone moieties (presumably semiquinone or benzoquinone) are able to oxidize Fe(II). Because no Fe(II) oxidation is observed in solutions containing benzoquinone at concentrations comparable to those used or measured here (data not shown), the Fe(II) oxidant is most likely the semiquinone radical ($Q^{\bullet-}$), which is formed as a result of oxidation of hydroquinone by Fe(III) (eq 1).

$$H_2Q + Fe(III) \underset{k_{-1}}{\overset{k_1}{\rightleftharpoons}} Q^{\bullet-} + Fe(II) \quad (1)$$

3.2. Benzoquinone Formation on Fe(III) Reduction by Hydroquinone. As shown in Figure 1b, the concentration of

DOI: 10.1021/acs.est.5b03189
Environ. Sci. Technol. 2015, 49, 14076−14084

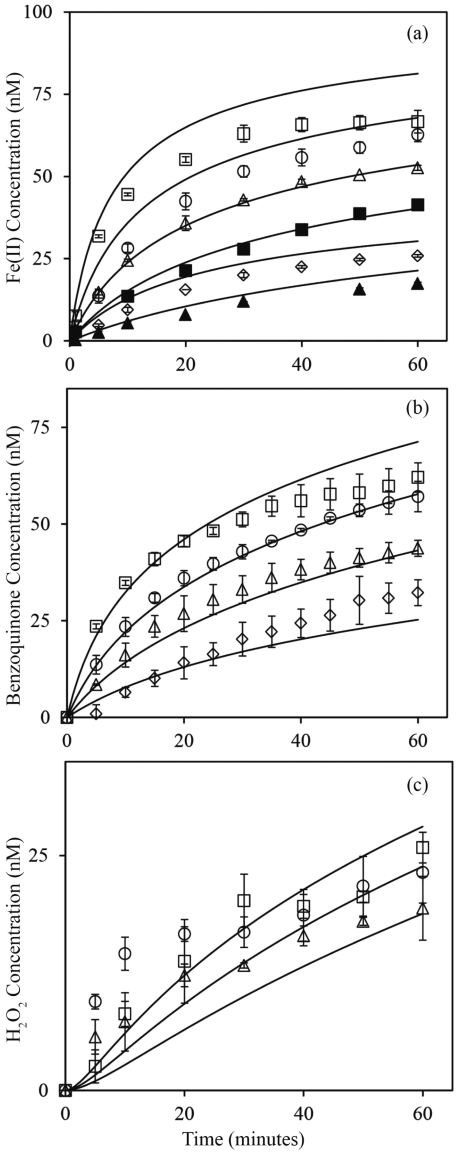

Figure 1. (a) Generation of Fe(II) as a result of the reduction of 100 nM Fe(III) in air-saturated solution containing 100 nM (closed triangles), 250 nM (closed squares), 500 nM (open triangles), 1 μM (open circles), and 2 μM (open squares) hydroquinone. Open diamonds indicate Fe(II) generated on the reduction of 50 nM Fe(III) by 500 nM hydroquinone in air-saturated solution at pH 4. (b) Generation of benzoquinone as a result of reduction of Fe(III) in air-saturated pH 4 solution containing 500 nM (triangles), 1 μM (circles), and 2 μM (squares) hydroquinone with 100 nM Fe(III) and 50 nM Fe(III) with 500 nM hydroquinone (diamonds) at pH 4. (c) Generation of H_2O_2 in air-saturated pH 4 solution containing 500 nM (triangles), 1 μM (circles), and 2 μM (squares) hydroquinone and 100 nM Fe(III). Symbols are experimental data (average of duplicate measurements); lines are model-predicted values.

benzoquinone increased over time in air-saturated solutions containing Fe(III) and H_2Q at pH 4. An increase in Fe(III) concentration results in an increase in the concentration of Q generated, suggesting that benzoquinone formation is due to the presence of Fe(III). No benzoquinone generation is observed in hydroquinone solution in the absence of Fe(III) (data not shown), in accord with the recognition that autoxidation of H_2Q is spin-restricted and very slow under acidic conditions.[18] The presence of Fe(III) overcomes the spin restriction and catalyzes the oxidation of H_2Q as shown in previous studies on the trace-metal-mediated oxidation of hydroquinone.[6,7,19] Although nearly complete oxidation of H_2Q was observed in the presence of Cu(II) under circumneutral pH conditions,[7] only a small fraction of H_2Q was oxidized under the acidic conditions investigated here, which is consistent with the rate law for the metal-catalyzed oxidation of hydroquinone being proportional to $[H^+]^{-1}$, indicating that, rather than the protonated form H_2Q, the monoanion HQ^- is the important species in this redox reaction.[20]

The stoichiometry of Q formation to Fe(II) formation at pH 4 is approximately 1:1 (see Table S1), which suggests that either (i) there exists an additional oxidant of $Q^{\bullet-}$ apart from Fe(III) (eq 2) or $Q^{\bullet-}$ via disproportionation reaction (eq 3) or (ii) there are additional sink(s) of Fe(II) apart from $Q^{\bullet-}$ and Q (as indicated in eqs 1 and 2). Given that no oxidation of Fe(II) was observed by dioxygen (which is the only expected sink of Fe(II) apart from quinone species in our experimental matrix), this suggests that Q formation occurs via reaction sequence, whereby $Q^{\bullet-}$ formed in the reaction shown in eq 1 is oxidized by dioxygen to form Q (eq 4). This mechanism of Q formation is further supported by the observation that partial deoxygenation (~90%) of the solution results in complete inhibition of Q generation (Figure 2).

$$Q^{\bullet-} + \mathrm{Fe(III)} \underset{k_{-2}}{\overset{k_2}{\rightleftharpoons}} \mathrm{Fe(II)} + Q \tag{2}$$

$$Q^{\bullet-} + Q^{\bullet-} + 2H^+ \underset{k_{-3}}{\overset{k_3}{\rightleftharpoons}} Q + H_2Q \tag{3}$$

$$Q^{\bullet-} + O_2 \underset{k_{-4}}{\overset{k_4}{\rightleftharpoons}} Q + HO_2^{\bullet} \tag{4}$$

A lack of Q generation in partially deoxygenated solution further supports that Q formation via $Q^{\bullet-}$ oxidation by Fe(III) (eq 2) or $Q^{\bullet-}$ disproportionation (eq 3) is negligible at least over the time scale, concentration, and pH of our experiments. Although oxidation of $Q^{\bullet-}$ by Fe(III) is reported to occur under circumneutral pH conditions' it may not occur at comparable rates under acidic conditions, given that the redox potential of the $Q^{\bullet-}$–H_2Q redox couple and the Q–$Q^{\bullet-}$ redox couple increases with a decrease in pH (see Figure S6), making $Q^{\bullet-}$ a better oxidant than reductant at lower pHs. The disproportionation of semiquinone radicals is most likely unimportant as a result of both the limited generation of $Q^{\bullet-}$ and its rapid removal by dioxygen and Fe(II).

Direct two-electron oxidation of H_2Q by Fe(III) resulting in formation of Q is also expected to be negligible because the formation of Q by such a pathway should be dioxygen-independent and should result in Fe(II) and Q formation in 2:1 stoichiometry, neither of which are consistent with our observation.

3.3. Generation of H_2O_2 on Fe(III) Reduction by Hydroquinone. As shown in Figure 1c, H_2O_2 is generated on addition of Fe(III) to air-saturated H_2Q solutions at pH 4, with the concentration of H_2O_2 generated increasing slightly with an increase in H_2Q concentration. H_2O_2 generation in these solutions occurs due to disproportionation of the superoxide (eq 5) formed upon the oxidation of $Q^{\bullet-}$ by O_2 (eq 4). Because the stoichiometry of Q to H_2O_2 generation is slightly less than 2:1 (Table S1), it appears that a small amount of $HO_2^{\bullet}$ decays via a pathway does not result in H_2O_2 production. Although the nature of this loss pathway is not

DOI: 10.1021/acs.est.5b03189
Environ. Sci. Technol. 2015, 49, 14076−14084

Figure 2

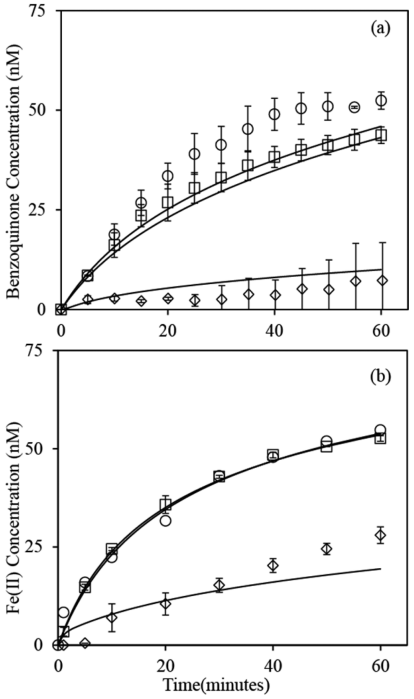

Figure 2. (a) Generation of benzoquinone in solutions containing 100 nM Fe(III) and 500 nM hydroquinone in air-saturated solution (squares), partially deoxygenated solution (diamonds), and in air-saturated solution containing 25 kU.L^{-1} SOD (circles) at pH 4. (b) Generation of Fe(II) in solutions containing 100 nM Fe(III) and 500 nM hydroquinone in air-saturated solution (squares), partially deoxygenated solution (diamonds), and in air-saturated solution containing 25 kU.L^{-1} SOD (circles) at pH 4. Symbols are experimental data (average of duplicate measurements); lines are model-predicted values.

clear from our experimental results, possibilities include the reduction of semiquinone (eq 6), Fe(III) (eq 7), or benzoquinone (eq 4) by superoxide.

$$HO_2^\bullet + HO_2^\bullet \xrightarrow{k_{disp}} O_2 + H_2O_2 \quad (5)$$

$$Q^{\bullet-} + HO_2^\bullet \xrightarrow{H^+} H_2Q + O_2 \quad (6)$$

$$Fe(III) + HO_2^\bullet \underset{k_{-7}}{\overset{k_7}{\rightleftharpoons}} Fe(II) + O_2 \quad (7)$$

3.4. Role of Dioxygen. Both Fe(II) and Q formation during H_2Q oxidation by Fe(III) at pH 4 is significantly ($p < 0.001$ using single-tailed Student's *t*-test) reduced in partially deoxygenated (~90%) solutions. This effect of dioxygen removal on Q formation provides confirmation that Q is indeed formed via the oxygenation of $Q^{\bullet-}$, and the decrease in rate and extent of Fe(II) formation presumably arises as a result of an increase in the steady-state concentration of $Q^{\bullet-}$ and concomitant increase in the rate of Fe(II) oxidation by $Q^{\bullet-}$ upon decrease in dioxygen concentration. The overall effect of removal of dioxygen is more pronounced on Q than Fe(II) formation, with the stoichiometric generation of Fe(II) to benzoquinone generation increasing from 1:1 in air-saturated solution to ~4:1 in partially deoxygenated solution. No H_2O_2 generation was observed in partially deoxygenated solution (data not shown), supporting the conclusion that H_2O_2 formation occurs principally via dioxygen reduction through the formation of superoxide.

3.5. Role of Superoxide. The role of superoxide in Fe(II) and Q generation was examined by adding SOD, which catalyzes the disproportion of superoxide to O_2 and H_2O_2. As shown in Figure 2, SOD has no significant effect ($p > 0.1$ using a single-tailed Student's *t*-test) on either Fe(II) generation or Q generation in air-saturated solution at pH 4, indicating that superoxide-mediated H_2Q oxidation[18] and superoxide-mediated Fe redox transformations[22] are unimportant under acidic conditions. The latter result is in contrast with the findings of earlier work, in which inorganic Fe(III) reduction and Fe(II) oxidation by superoxide occurred rapidly under acidic conditions.[22] As confirmed later, the lack of effect of SOD addition on Fe(II) generation observed here is due to the fact that the forward Fe(III) reduction by $HO_2^\bullet$ (eq 7) balances the backward Fe(II) oxidation by $HO_2^\bullet$ (eq 8), thereby resulting in zero-net Fe(II) generation by $HO_2^\bullet$ but catalytic disproportionation of $HO_2^\bullet$. We will also show that even though $HO_2^\bullet$ can reduce $Q^{\bullet-}$ and Q, these are important reactions with respect to the fate of $HO_2^\bullet$, but they play a minor role in controlling the fate of $Q^{\bullet-}$ and Q with the result that SOD addition has minimal effect on Q generation.

$$Fe(II) + HO_2^\bullet \xrightarrow{H^+} Fe(III) + H_2O_2 \quad (8)$$

3.6. Effect of pH. As shown in Figure 3a, an increase in pH results in a decrease in the concentration of Fe(II) generated on Fe(III) reduction by H_2Q, with Fe(II) concentration generated after 60 min being 2-fold higher at pH 4 than at pH 5. This suggests that the Fe(III) reduction rate decreases and Fe(II) oxidation rate increases with an increase in pH. Benzoquinone generation decreases slightly with increase in pH (Figure 3b), which is consistent with the observed effect of pH on Fe(II) generation (Figure 3a). With an increase in pH, the overall extent of Fe(II) and $Q^{\bullet-}$ generation via the reactions shown in eq 1 decreases, which further results in decreased Q generation via the oxidation of $Q^{\bullet-}$. H_2O_2 generation increases slightly with an increase in pH in the pH range 3–5; however, the difference in H_2O_2 generation rate at pH 4 and 5 is not significant ($p > 0.1$ using single-tailed Student's *t*-test; Figure 3c).

The stoichiometry for Fe(II) to Q generation is slightly higher than 1:1, and the stoichiometry for Q to H_2O_2 generation is slightly less than 2:1 at pH 3 (see Table S1), which is similar to that observed at pH 4. The stoichiometry for Fe(II) to Q generation is approximately 1:1, and the stoichiometry for Q to H_2O_2 generation is slightly less than 2:1 at pH 4.5 (Table S1), which is the same as that observed at pH 4. The same effect of dioxygen removal and SOD addition on Fe(II) and Q generation is observed at pH 3, 4, and 4.5 (Figures S3 and S4), thereby supporting the conclusion that the same reactions occur at these pHs.

Because the oxygenation of Fe(II) is important at pH 5 (see Figure S2), the stoichiometry of Fe(II) to Q generation is less than 1:1, and the stoichiometry of Q:H_2O_2 generation is more than 2:1 at this pH. The oxygenation of Fe(II) in addition to its oxidation by the semiquinone radical results in a net decrease in Fe(II) generation and increase in H_2O_2 generation. Although the oxygenation of Fe(II) occurs, Fe(II) oxidation by $Q^{\bullet-}$ is still the main pathway for Fe(II) oxidation at pH 5 because the partial removal of dioxygen results in decreased Fe(II) generation (Figure S3).

DOI: 10.1021/acs.est.5b03189
Environ. Sci. Technol. 2015, 49, 14076–14084

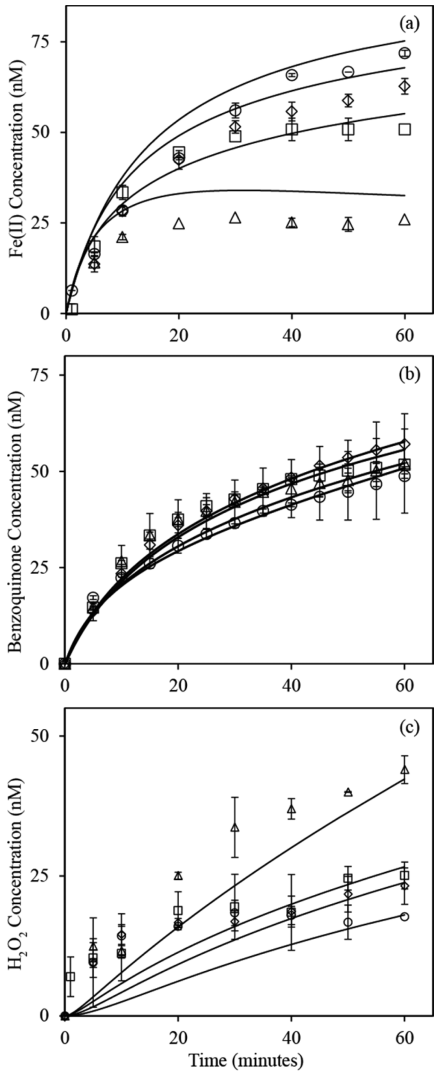

Figure 3. Generation of (a) Fe(II), (b) benzoquinone, and (c) H_2O_2 as a result of 100 nM Fe(III) reduction at pH 3 (circles), pH 4 (diamonds), pH 4.5 (squares), and pH 5 (triangles) in the presence of 1 μM hydroquinone solution. Symbols are experimental data (average of duplicate measurements); lines are model-predicted values. More experimental results on Fe(II) and Q generation in the presence of other concentration of hydroquinone are shown in Figure S3. All experiments were performed in air-saturated solution.

3.7. Thermodynamic Considerations Relating to the Reduction of Fe(III) by H_2Q. Global thermodynamics calculations assuming equilibrium between the Fe(III)−Fe(II) redox couple and the Q−H_2Q redox couple results in the predicted concentrations and stoichiometry of Fe(II) and Q that are inconsistent with the measured concentrations of these parameters, with this result providing further support for our conclusion that the direct two-electron oxidation of H_2Q by Fe(III) or the sequential two-electron oxidation of H_2Q by Fe(III) does not occur to an appreciable extent at the pH and time-scale employed in this study. Thermodynamic calculations performed assuming (i) equilibrium between the Fe(III)−Fe(II) and the H_2Q−$Q^{\bullet-}$ redox couples and (ii) equilibrium between the $Q^{\bullet-}$−Q and O_2−$HO_2^{\bullet}$ redox couples results in ΔG close to zero, supporting the conclusion that quasi-equilibrium between these four redox couples exists (see section S5 in the Supporting Information for details of this calculation) as depicted in the reaction schematic shown in Figure 4. This observation further suggests that the ratio of the rate constant

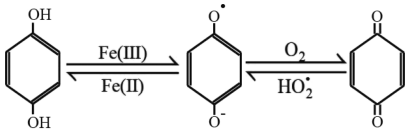

Figure 4. Reaction schematic showing the equilibria between various quinone species in the presence of Fe in air-saturated solution.

for the forward reaction (i.e., k_1) and the backward reaction (i.e., k_{-1}) is related to the ΔE^0 for the reactions shown in eq 1, calculated using the reported redox potential (E^0) for the Fe(III)−/Fe(II) and $Q^{\bullet-}$−H_2Q redox couples. Similarly, the ratio of the forward and backward rate constants for the reactions shown in eq 4 (i.e., k_4/k_{-4}) is calculated using E^0 for the Q−$Q^{\bullet-}$ and E^0 O_2−$HO_2^{\bullet}$ redox couples. These calculated values of the equilibrium constants ($K_{H_2Q\text{-}Fe(III)}$ and $K_{Q^{\bullet-}-O_2}$) for these reactions are shown in Table S4 (see section S5 in the Supporting Information for details on calculation of these values) and are used as thermodynamic constraints in the kinetic modeling of our experimental results as described in the following section.

3.8. Kinetics and Mechanism of Fe(III) and Hydroquinone Interaction. The kinetic model showing the proposed Fe(III) and hydroquinone interactions is shown in Table 1. The rate constant for the reduction of Fe(III) by hydroquinone (k_1; reaction 1; Table 1) was determined on the basis of the best fit to the measured rate and the extent of Fe(II) generation and was found to be pH-independent. The pH-dependent rate constants for oxidation of Fe(II) by semiquinone (k_{-1}; reaction 1; Table 1) and the rate constants for the oxidation of semiquinone radicals by dioxygen (k_4; reaction 4; Table 1) were determined on the basis of the best fit to the measured rate and extent of Fe(II) and Q generation and with the thermodynamic constraint that $k_{-1} = k_1/K_{H_2Q-Fe(III)}$ imposed (as mentioned in section 3.7).

As discussed, the oxidation of $Q^{\bullet-}$ by Fe(III) (reaction 2; Table 1) is unimportant in the conditions of our experiments due to the decrease in reduction capacity of $Q^{\bullet-}$ that occurs at lower pHs, as indicated by increased redox potential of the Q−$Q^{\bullet-}$ couple under acidic conditions (see Figure S6). Furthermore, under acidic conditions, the redox potential of the $Q^{\bullet-}$/QH_2 couple increases, making $Q^{\bullet-}$ a better oxidant than reductant under acidic conditions (Figure S6). Similarly, the oxidation of Fe(II) by Q (reaction 2, Table 1), which is reported to occur with other trace metals such as Cu under circumneutral pH conditions,[7,23] and the resultant catalysis of comproportionation reaction is also determined to be unimportant at the time-scale and pH investigated here due to the limited generation of Q. Our kinetic modeling further shows that the inclusion of this reaction using rate constants of $\leq 1 \times 10^5$ and $\leq 1 \times 10^3$ M^{-1} s^{-1} for k_2 and k_{-2}, respectively, does not affect the model output. The value of k_{-2} used here is 10-fold higher than the reported value,[7] supporting the premise that the oxidation of Fe(II) by Q is unimportant due to the limited generation of Q. Although the value of k_2 (1×10^5 M^{-1} s^{-1}) used here is lower than the value reported for the Fe(III) cytochrome-semiquinone reaction at pH 7,[21] it is possibly due to variation in the redox potential and speciation of $Q^{\bullet-}$ with change in pH. The semiquinone radical is mostly present in the

DOI: 10.1021/acs.est.5b03189
Environ. Sci. Technol. 2015, 49, 14076−14084

Table 1. Kinetic Model for Hydroquinone-Mediated Reduction of Fe(III) in the pH Range of 3−5[a]

no.	reaction		rate constant ($M^{-1}S^{1-}$)				reference
			pH 3	pH 4	pH 4.5	pH 5	
1	$H_2Q + Fe(III) \underset{k_{-1}}{\overset{k_1}{\rightleftharpoons}} Q^{\bullet-} + Fe(II)$			-----k_1 = 1×10^3-----			9
		k_{-1}	2.4×10^6	4×10^6	7×10^6	9×10^6	–
2	$Q^{\bullet-} + Fe(III) \underset{k_{-2}}{\overset{k_2}{\rightleftharpoons}} Fe(II) + Q$			-----k_2 ≤ 1×10^5-----			21
				-----k_{-2} ≤ 1×10^3-----			7
3	$Q^{\bullet-} + Q^{\bullet-} + 2H^+ \underset{k_{-3}}{\overset{k_3}{\rightleftharpoons}} Q + H_2Q$			-----k_3 ≤ 1×10^{10}-----			21,7
				-----k_{-3} ≤ 8×10^7-----			21,7
4	$Q^{\bullet-} + O_2 \underset{k_{-4}}{\overset{k_4}{\rightleftharpoons}} Q + HO_2^{\bullet}$	k_4	5×10^2	7×10^2	9×10^2	1×10^3	21,27
		k_{-4}	1.8×10^6	4×10^6	8×10^6	1.9×10^7	27
5	$HO_2^{\bullet} + HO_2^{\bullet} \xrightarrow{k_{disp}} O_2 + H_2O_2$	k_{disp}	2×10^6	1.1×10^7	2×10^7	2.5×10^7	26
6	$Q^{\bullet-} + HO_2^{\bullet} \xrightarrow{k_6} H_2Q + O_2$			-----k_6 = 5×10^8-----			–
7	$Fe(III) + HO_2^{\bullet} \underset{k_{-7}}{\overset{k_7}{\rightleftharpoons}} Fe(II) + O_2$	k_7	5×10^5	9×10^5	1.4×10^6	2.5×10^6	22
		k_{-7}	–	–	–	1.3	–
8	$Fe(II) + HO_2^{\bullet} \xrightarrow{k_8} Fe(III) + H_2O_2$	k_8	1.3×10^6	2.4×10^6	4.1×10^6	6.6×10^6	22

[a]Important reactions are highlighted.

deprotonated form at pH 7, and it exists in both deprotonated ($Q^{\bullet-}$) and protonated ($HQ^{\bullet}$) forms under acidic conditions. Because $HQ^{\bullet}$ is expected to be less reactive than $Q^{\bullet-}$,[7] the rate constant of Fe(III)-semiquinone reaction decreases under acidic conditions. Furthermore, as discussed, variation in the redox potential of $Q^{\bullet-}$ with change in pH is also expected to affect its reactivity as reductant, with resultant decrease in the rate of oxidation of $Q^{\bullet-}$ by Fe(III). Although this reaction was determined to be unimportant at the time scales of our experiments, it may play an important role in Q generation in the complete absence of dioxygen on longer time-scales.

Disproportionation of the semiquinone radical (reaction 3, Table 1) is also unimportant in the experimental system investigated here as a result of the low steady-state concentrations of the semiquinone radical present. The comproportionation reaction between H_2Q and Q (reaction 3, Table 1) was also not important in the system investigated here as a result of the extremely low concentrations of the doubly deprotonated hydroquinone species (Q^{2-}) (the reported active species toward comproportionation[21,24,25]) with concentrations of $\sim 10^{-13}$−10^{-15} M in the pH 5−3 solutions used in this study. Furthermore, the concentration of Q is also very small ($\sim 10^{-8}$ M), supporting the conclusion that the comproportionation reaction is unimportant in our system. The results of our kinetic modeling further show that the inclusion of the comproportionation reaction and the semiquinone disproportionation reaction does not have any effect on the model output, even when the rate constants for these reactions are $>1 \times 10^{10}$ and $\leq 8 \times 10^7$ M^{-1} s^{-1}, respectively.

The pH-dependent rate constant for superoxide disproportionation (k_{disp}; reaction 5; Table 1) reported by Bielski and coworkers[26] was used here. The reduction of $Q^{\bullet-}$ and Q by superoxide (reactions 6 and 4, respectively; Table 1) were included in the model to account for superoxide loss via pathways other than the disproportionation reaction, with the rate constants for these reactions determined on the basis of the best fit to the H_2O_2 concentration data and the effect of SOD addition on Fe(II) generation. However, the rate constant for oxidation of superoxide by semiquinone (reaction 6; Table 1) is not well-constrained by our kinetic model due to its minor role in controlling the Fe(II) and Q generation rates. Although the reaction of Q with superoxide (reaction 4, Table 1) plays a minor role in affecting the model output, the rate constant for this reaction (k_{-4}) is well-constrained by the relationship $k_{-4} = k_4/K_{Q^{\bullet-}-O_2}$ (see section 3.7). We have also included $HO_2^{\bullet}$-mediated Fe(II) oxidation and Fe(III) reduction (reactions 7 and 8) with rate constants similar to the values reported by Rush and Bielski;[22] however, these reactions do not play an important role in Fe(II) generation in the pH range of 3−5, as confirmed by the model-predicted effect of SOD addition (Figures 2 and S4).

The rate of Fe(II) oxidation by dioxygen (reaction 7, Table 1) is extremely slow at pH < 5 (see Figure S1) and therefore neglected. However, at pH 5, oxygenation of Fe(II) becomes important ($t_{1/2}$ < 1 h) and is therefore included in the kinetic model. The rate constant for this reaction (k_{-7}) at pH 5 was determined on the basis of the best fit to the H_2O_2 generation data and Fe(II) oxygenation rate observed in pH 5 solution; however, the value at other pHs investigated here could not be determined.

As shown in Table 1, the rate constant for some reactions are pH-dependent due to changes in the speciation of the entities involved in these reactions. Although the speciation of Fe(III) varies in the pH range investigated here (see Figure S5), the rate constant for the Fe(III) and H_2Q reaction (reaction 1; Table 1) based on our experimental data is similar under all conditions examined. This result suggests that the reactivity of $FeOH^{2+}$ and $Fe(OH)_2^+$ (the two dominant Fe(III) species in our experimental matrix) are similar, thereby resulting in the same Fe(III) reduction rate under all pH conditions investigated here. This is consistent with earlier studies of Fe(III) reduction by superoxide, which reported that all Fe(III) species have similar reactivity toward superoxide, with the experimentally determined rate constant for reduction of $FeSO_4^+$ and $FeOH^{2+}$ by O_2^- being similar (1.5×10^8 M^{-1} s^{-1}).[22] The rate constant for the oxidation of Fe(II) by $Q^{\bullet-}$ is pH-dependent (k_{-1}; Table 1) because the form of the semiquinone radical (with pK_a= 4.1) changes over the pH range investigated. As reported earlier,[7] the deprotonated form, $Q^{\bullet-}$, is a more active oxidant than $HQ^{\bullet}$ and therefore oxidizes

DOI: 10.1021/acs.est.5b03189
Environ. Sci. Technol. 2015, 49, 14076−14084

Fe(II) more rapidly than the protonated form, with resultant decrease in the concentration of Fe(II) and Q formed at higher pHs. As shown in eq 9, the overall rate constant of Fe(II) oxidation is a function of the fraction of the protonated and deprotonated species at each pH, i.e.,

$$k_{-1} = \alpha_0 k_{-1}^{HQ} + \alpha_1 k_{-1}^{Q^{\bullet-}} \quad (9)$$

where $\alpha_0 = ([H^+]/([H^+] + K_{HQ}))$; $\alpha_1 = 1 - \alpha_0$; $K_{HQ} = 10^{-4.1}$; $k_{-1}^{HQ} = 2 \times 10^6\ M^{-1}\ s^{-1}$, and $k_{-1}^{Q^{\bullet-}} = 1 \times 10^7\ M^{-1}\ s^{-1}$

The rate constant for oxygenation of the semiquinone radical (reaction 4; Table 1) also increases with an increase in pH due to the higher reactivity of $Q^{\bullet-}$ than $HQ^{\bullet}$. The variation in this rate constant with pH is also modeled as a function of the speciation of the semiquinone radical and is given by the following equation:

$$k_4 = \alpha_0 k_4^{HQ} + \alpha_1 k_4^{Q^{\bullet-}} \quad (10)$$

where $\alpha_0 = ([H^+]/([H^+] + K_{HQ}))$, $\alpha_1 = 1 - \alpha_0$, $K_{HQ} = 10^{-4.1}$, k_4^{HQ} $4.6 \times 10^2\ M^{-1}\ s^{-1}$, and $k_4^{Q^{\bullet-}} = 1.0 \times 10^3\ M^{-1}\ s^{-1}$. The model-predicted rate constant for the semiquinone oxygenation reaction is slightly lower than that reported under alkaline conditions (for example, Yuan et al.[7] report a value of 1.0×10^4 $M^{-1}\ s^{-1}$ at pH 8.0).

The pH-dependence of the rate constant for superoxide disproportionation (reaction 5; Table 1) is modeled as a function of the speciation of superoxide as described earlier;[26] i.e.,

$$k_{disp} = \alpha_0 \alpha_0 k_{HO_2^{\bullet}} + \alpha_0 \alpha_1 k_{O_2^-} \quad (11)$$

where $\alpha_0 = ([H^+]/([H^+] + K_{HO_2^{\bullet}}))$, $\alpha_1 = 1 - \alpha_0$, $k_{HO_2^{\bullet}} = 8.3 \times 10^5\ M^{-1}\ s^{-1}$, $k_{O_2^-} = 9.7 \times 10^7\ M^{-1}\ s^{-1}$, and $K_{HO_2^{\bullet}} = 10^{-4.8}$

As reported earlier,[22] the rate constant of Fe(III) reduction by $HO_2^{\bullet}$ is very low ($<1 \times 10^3\ M^{-1}\ s^{-1}$), with most of the Fe(III) reduction by superoxide attributed to its reaction with O_2^-. Thus, the rate constant for Fe(III) reduction by superoxide (reaction 7; Table 1) determined on the basis of the best fit to our experimental results is shown to vary with pH due to the change in concentration of O_2^-; i.e.,

$$k_7 = \alpha_1 k_7^{O_2^-} \quad (12)$$

where $\alpha_1 = ([K_{HO_2^{\bullet}}]/([H^+] + K_{HO_2^{\bullet}}))$; k_7 represents the overall rate constant for reduction of Fe(III) by superoxide, $k_7^{O_2^-} = 1.5 \times 10^7\ M^{-1}\ s^{-1}$ and $K_{HO_2^{\bullet}} = 10^{-4.8}$. The value of $k_7^{O_2^-}$ determined here is 1-fold lower than the reported value of $1.5 \times 10^8\ M^{-1}\ s^{-1}$[22] under strongly acidic conditions (<pH 2) with a very high concentration of Fe(III) (~100 μM).

The rate constant for Fe(II) oxidation by superoxide (reaction 8; Table 1) varies with pH due to the difference in reactivity of O_2^- and $HO_2^{\bullet}$ as reported earlier;[22] i.e.,

$$k_8 = \alpha_0 k_8^{HO_2^{\bullet}} + \alpha_1 k_8^{O_2^-} \quad (13)$$

where $\alpha_0 = ([H^+]/([H^+] + K_{HO_2^{\bullet}}))$ and $\alpha_1 = 1 - \alpha_0$; k_8 represents the overall rate constant for oxidation of Fe(II) by superoxide; $k_8^{HO_2^{\bullet}} = 1.2 \times 10^6\ M^{-1}\ s^{-1}$, $k_8^{O_2^-} = 1.0 \times 10^7\ M^{-1}\ s^{-1}$, and $K_{HO_2^{\bullet}} = 10^{-4.8}$.

As shown in Figures 1−3, S3, S4, and S5, the model provides a good description of the experimental results obtained here, with the kinetic model predicting the effect of dioxygen removal, SOD addition, and pH reasonably well. Because Fe continually cycles between the +III and +II oxidation states in the presence of H_2Q, the turnover frequency (TOF) at steady-state can be deduced from the kinetic model developed here using the expressions:

$$TOF = \frac{\text{Fe(III) reduction rate}}{\text{total Fe concentration}} \quad (14)$$

and

$$\begin{aligned}\text{Fe(III) reduction rate} &= k_1[\text{Fe(III)}]_{ss}[H_2Q]_{ss} \\ &= k_1(Fe_0 - [\text{Fe(II)}]_{ss})(Q_0 - [Q]_{ss})\end{aligned} \quad (15)$$

where $k_1 = 1 \times 10^3\ M^{-1}\ s^{-1}$ and Fe_0 and Q_0 represent the initial Fe(III) and H_2Q concentrations, respectively. The $[\text{Fe(II)}]_{ss}$ and $[Q]_{ss}$ values were determined from the kinetic model.

The calculated TOF increases with increase in pH as a result of the higher rates of Fe(II) oxidation at higher pHs with values of 0.73, 1.23, 2.22, and 4.41 h^{-1}, deduced for 2 μM H_2Q solutions at pH 3, 4, 4.5, and 5, respectively.

4. ENVIRONMENTAL IMPLICATIONS

Our results show that hydroquinone reduces Fe(III) resulting in formation of Fe(II) and semiquinone radicals. The semiquinone radicals so formed subsequently oxidize Fe(II) to Fe(III). The oxidation rate of Fe(II) by semiquinone radicals increases with an increase in pH due to the speciation change of semiquinone radicals, with its deprotonated form ($Q^{\bullet-}$) oxidizing Fe(II) more rapidly than the protonated form ($HQ^{\bullet}$). The rapid redox cycling of Fe between the +III and +II oxidation states in the presence of H_2Q is accompanied by the generation of benzoquinone and reactive oxygen species (particularly $HO_2^{\bullet}$ and H_2O_2), with O_2 playing an important role in these redox transformations.

As noted earlier, quinone moieties are recognized to be responsible, to a large extent, for the redox behavior of NOM. Indeed, the results presented here showing the interplay between iron and quinone species bear many similarities, as well as some striking differences, to the results of recent studies of the interaction of Fe(II) and Fe(III) with SRFA.[9] Of particular note, as shown in Figure 5, is the 100- to 1000-fold lower estimated steady-state concentration of the semiquinone radical in solutions of 1,4-hydroquinone compared to those in SRFA solutions containing comparable concentrations of hydroquinone-like moieties. The substantially higher steady-

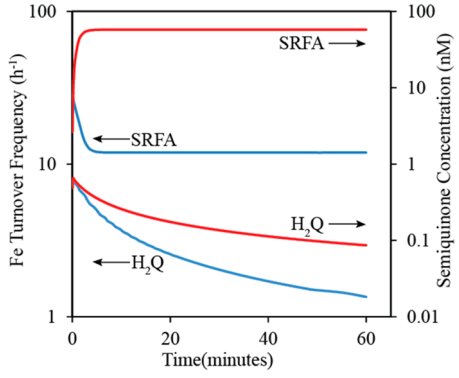

Figure 5. Comparison of turnover frequency and semiquinone concentration in air-saturated solution containing SRFA and 1,4-hydroquinone in the presence of 100 nM Fe(III) and 2 μM hydroquinone at pH 4.

DOI: 10.1021/acs.est.5b03189
Environ. Sci. Technol. 2015, 49, 14076−14084

state concentration of the semiquinone in SRFA is most likely a consequence of the ability of the unpaired electron on the semiquinone radical in this large molecule to be stabilized by both delocalization over an array of conjugated aromatic carbons and the presence of electron-donating alkyl groups. The increased stability of semiquinone radicals in SRFA solution compared to that in pure hydroquinone solution make it a substantially more effective Fe(II) oxidant than is the case in the simpler quinone, with the result that quinone moieties present in SRFA are expected to play a much more important role in Fe redox transformations compared to that of pure hydroquinone solutions. This is reflected in the differences in Fe turnover frequencies shown in Figure 5, with Fe cycling between the +III and +II oxidation states in SRFA at 10−100 times the rate observed in pure 1,4-hydroquinone solution. Although notable differences are observed between simple hydroquinone and quinone moieties found in SRFA, it is possible that more complex quinone compounds, particularly those with alkyl substitution or those with the potential for a high degree of electron delocalization, may behave in a manner similar to NOM.

We therefore conclude that, while quinone moieties are recognized to be principally responsible for the redox properties of NOM, care should be taken in extrapolating the results observed in pure quinone solutions to the natural aquatic environment. In particular, the unique stability of the semiquinone radical in the highly conjugated and substituted environment of NOM will have strong implications for the rate and extent of metal redox transformations as well as reactive oxygen species generation in natural aquatic systems, with the latter being of relevance to both the oxidative degradation of the NOM itself and any other organic compounds associated with it.

■ ASSOCIATED CONTENT

Supporting Information

The Supporting Information is available free of charge on the ACS Publications website at DOI: 10.1021/acs.est.5b03189.

Details of reagent preparation; deoxygenation experimental procedures; pH control; effect of pH on speciation; speciation, ΔG, and equilibrium constant calculations; sensitivity analysis of the kinetic model. Figures showing Fe(II) generation and decay in the dark at various pH and in various solutions, benzoquinone generation in various solutions at various pH, variation in speciation with change in pH, E_H/pH for various redox couples, and sensitivity analysis of model reactions. Tables showing the concentration of Fe(II), benoquinone, and H_2O_2 formed in air-saturated solution on addition of H_2Q and Fe(III), calculated equilibrium concentrations and ΔG values, and principle component analysis. (PDF)

■ AUTHOR INFORMATION

Corresponding Author

*Tel. +61-2-9385 5060; fax +61-2-9385 6139; e-mail: d.waite@unsw.edu.au.

Notes

The authors declare no competing financial interest.

■ ACKNOWLEDGMENTS

Funding for this work was provided by an Australian Research Council (ARC) Discovery Early Career Researcher Award (DECRA) to S.G., an Australian Postgraduate Award to C.J., and an ARC Discovery Grant DP120103234 to T.D.W. and colleagues. Assistance provided by Dr. Christopher Miller in reviewing a penultimate version of this manuscript and in refining a number of the figures presented is gratefully acknowledged.

■ REFERENCES

(1) Thorn, K. A.; Arterburn, J. B.; Mikita, M. A. 15N and 13C NMR investigation of hydroxylamine-derivatized humic substances. *Environ. Sci. Technol.* **1992**, *26* (1), 107−116.

(2) Fimmen, R. L.; Cory, R. M.; Chin, Y. P.; Trouts, T. D.; McKnight, D. M. Probing the oxidation-reduction properties of terrestrially and microbially derived dissolved organic matter. *Geochim. Cosmochim. Acta* **2007**, *71*, 3003−3015.

(3) Cory, R. M.; McKnight, D. M. Fluorescence spectroscopy reveals ubiquitous presence of oxidized and reduced quinones in dissolved organic matter. *Environ. Sci. Technol.* **2005**, *39*, 8142−8149.

(4) Aeschbacher, M.; Sander, M.; Schwarzenbach, R. P. Novel electrochemical approach to assess the redox properties of humic substances. *Environ. Sci. Technol.* **2010**, *44* (1), 87−93.

(5) Garg, S.; Rose, A. L.; Waite, T. D. Photochemical production of superoxide and hydrogen peroxide from natural organic matter. *Geochim. Cosmochim. Acta* **2011**, *75* (15), 4310−4320.

(6) Uchimiya, M.; Stone, A. T. Redox reactions between iron and quinones: Thermodynamic constraints. *Geochim. Cosmochim. Acta* **2006**, *70*, 1388−1401.

(7) Yuan, X.; Pham, a. N.; Miller, C. J.; Waite, T. D. Copper-catalyzed hydroquinone oxidation and associated redox cycling of copper under conditions typical of natural saline waters. *Environ. Sci. Technol.* **2013**, *47*, 8355−8364.

(8) Garg, S.; Ito, H.; Rose, A. L.; Waite, T. D. Mechanism and kinetics of dark iron redox transformations in previously photolyzed acidic natural organic matter solutions. *Environ. Sci. Technol.* **2013**, *47*, 1861−1869.

(9) Garg, S.; Jiang, C.; Waite, T. D. Mechanistic insights into iron redox transformations in the presence of natural organic matter: Impact of pH and light. *Geochim. Cosmochim. Acta* **2015**, *165*, 14−34.

(10) Senesi, N. Molecular and quantitative aspects of the chemistry of fulvic acid and its interactions with metal ions and organic chemicals. Part I. The electron spin resonance approach. *Anal. Chim. Acta* **1990**, *232* (1), 51−75.

(11) Senesi, N. Molecular and quantitative aspects of the chemistry of fulvic acid and its interactions with metal ions and organic chemicals. Part II. *Anal. Chim. Acta* **1990**, *232* (1), 77−106.

(12) Stookey, L. L. Ferrozine—a new spectrophotometric reagent for iron. *Anal. Chem.* **1970**, *42* (7), 779−781.

(13) Wilcoxen, J.; Zhang, B.; Hille, R. Reaction of the molybdenum- and copper-containing carbon monoxide dehydrogenase from oligotropha carboxydovorans with quinones. *Biochemistry* **2011**, *50* (11), 1910−1916.

(14) Zhou, M.; Diwu, Z.; Panchuk-Voloshina, N.; Haugland, R. P. A stable nonfluorescent derivative of resorufin for the fluorometric determination of trace hydrogen peroxide: applications in detecting the activity of phagocyte NADPH oxidase and other oxidases. *Anal. Biochem.* **1997**, *253* (253), 162−168.

(15) Garg, S.; Rose, A. L.; Waite, T. D. Pathways contributing to the formation and decay of ferrous iron in sunlit natural waters. *ACS Symp. Ser.* **2011**, *1071* (III), 153−176.

(16) Ianni, J. C. A comparison of the Bader−Deuflhard and the Cash−Karp Runge − Kutta integrators for the GRI-MECH 3.0 model based on the chemical kinetics code Kintecus. *Combustion* **2003**, *1* (3), 1368−1372.

DOI: 10.1021/acs.est.5b03189
Environ. Sci. Technol. 2015, 49, 14076−14084

(17) Vajda, S.; Valko, P.; Turányi, T. Principal component analysis of kinetic models. *Int. J. Chem. Kinet.* **1985**, *17* (1), 55−81.
(18) Roginsky, V.; Barsukova, T. Kinetics of oxidation of hydroquinones by molecular oxygen. Effect of superoxide dismutase. *J. Chem. Soc. Perkin Trans. 2* **2000**, *7*, 1575−1582.
(19) Miller, D. M.; Buettner, G. R.; Aust, S. D. Transition metals as catalysts of "autoxidation" reactions. *Free Radical Biol. Med.* **1990**, *8* (4), 95−108.
(20) Song, Y.; Buettner, G. R. Thermodynamic and kinetic considerations for the reaction of semiquinone radicals to form superoxide and hydrogen peroxide. *Free Radical Biol. Med.* **2010**, *49* (6), 919−962.
(21) Yamazaki, I.; Ohnishi, T. One-electron-transfer reactions in biochemical systems I. Kinetic analysis of the oxidation-reduction equilibrium between quinol-quinone and ferro-ferricytochrome c. *Biochim. Biophys. Acta, Biophys. Incl. Photosynth.* **1966**, *112* (3), 469−481.
(22) Rush, J. D.; Bielski, B. H. J. Pulse radiolytic studies of the reaction of HO2/O2- with iron(II)/iron(III) ions. The reactivity of HO2/O2- with ferric ions and its implication on the occurrence of the Haber-Weiss reaction. *J. Phys. Chem.* **1985**, *89* (23), 5062−5066.
(23) Yuan, X.; Miller, C. J.; Pham, a. N.; Waite, T. D. Kinetics and mechanism of auto- and copper-catalyzed oxidation of 1,4-naphthohydroquinone. *Free Radical Biol. Med.* **2014**, *71*, 291−302.
(24) Roginsky, V. a.; Pisarenko, L. M.; Bors, W.; Michel, C. The kinetics and thermodynamics of quinone−semiquinone−hydroquinone systems under physiological conditions. *J. Chem. Soc., Perkin Trans. 2* **1999**, *2*, 871−876.
(25) Rich, P. R.; Bendall, D. S. The kinetics and thermodynamics of the reduction of cytochrome c by substituted p-benzoquinols in solution. *Biochim. Biophys. Acta, Bioenerg.* **1980**, *592* (3), 506−518.
(26) Bielski, B.; Cabelli, D.; Arudi, R.; Ross, A. Reactivity of HO2/O2- Radicals in Aqueous Solution. *J. Phys. Chem. Ref. Data* **1985**, *14* (4), 1041−1100.
(27) Meisel, D. Free energy correlation of rate constants for electron transfer between organic systems in aqueous solutions. *Chem. Phys. Lett.* **1975**, *34* (2), 263−266.

DOI: 10.1021/acs.est.5b03189
Environ. Sci. Technol. 2015, 49, 14076−14084